Reply to Dr. Diego G. Miralles interactive comment

We would like to thank Dr. Diego G. Miralles for his constructive comments. We are generally in agreement with his sentiments. Most importantly, we agree that our original manuscript was overly aggressive in lumping various evapotranspiration (ET) estimation approaches into a single conceptual category. As Dr. Diego points out, there are important differences between these approaches that are relevant for the stated purposes of our paper.

Nevertheless, we would like to stress that all approaches considered in our paper contain (at their core) a parameterized relationship between soil water content (θ) and ET. While the implications of mis-parameterization this relationship are arguably more severe for a land surface model, we believe that this issue remains relevant for any approach (such as GLEAM) that utilizes a water balance (and/or data assimilation system) approach to estimate θ and, in turn, uses θ to constrain ET. Regardless of the complexity that a given approach employs, failing to accurately describe the relationship between ET and (large number of potential) environmental constraints should eventually degrade the robustness of the model. We believe that this is true regardless of whether a model is employed as a retrospective, diagnostic or predictive manner. Our paper is an attempt to "open the lid" on these models to measure internal θ/ET coupling and explore the impact of potential mis-coupling on ET estimation.

Given this emphasis, Diego's suggestion to expand our analysis to include direct flux validation is an excellent one. Indeed, preliminary results suggest that, despite its simplicity, GLEAM does not underperform more complex land surface models with respect to daily ET predictions. Therefore, as Diego points out, any criticism of GLEAM must be tempered by this bottom-line result.

Therefore, we've made the following changes to our current manuscript:

1. Change the characterization of GLEAM from a "land surface model" to "retrieval algorithm" throughout the revised manuscript and add a more complete discussion of differences in complexity and envisioned application for various modelling approaches.

2. Directly evaluate the GLEAM ET accuracy and better describe the connection between accurate θ/ET coupling and the absolute accuracy of GLEAM ET predictions. Pertinent revisions are presented in new Fig. 6 and the related discussions.

Reply to Referee #1 interactive comment

We would like to thank Referee #1 for the constructive comments.

I only have one comment for one issue which I think the authors should consider. In the study I did not find any particular discussion related to the type of vegetation characterizing the AmeriFlux sites and its effect on the result. I think that vegetation type can be relatively important as for example grass roots are shallower with respect to tree and shrub roots and thus can exert potential different effects both on the coupling strength between the soil moisture profile (surface vs. root zone) and on the transpiration flux itself also considering that transpiration is the dominant pathway for the total evapotranspiration and is estimated to account for two-thirds of global land ET based on flux tower measurements (Schlesinger and Jasechko,2014). Based on that the authors should provide at least a discussion on the potential effects of the vegetation type on the presented results.

Thanks for the comments. In order to minimize the effect of different root depths from different vegetation types on NMI(θ_S, fPET) and NMI(θ_V, fPET), we used exponential filter to extrapolate θ to a unified 40 cm bottom layer depth and find that the overall fPET information contained in θ_S is slightly higher than that of θ_V. However, the difference between NMI(θ_S, fPET) and NMI(θ_V, fPET) diminishes when using different methods for calculating θ_V using AmeriFlux observations.

We've added more extensive discussion regarding the role of vegetation on key results in the revised manuscript. In particular, Fig. 4 has been newly expanded to better isolate the impact of vegetation type and the role of vegetation types is now directly addressed via new text appearing in Section 3.3 of the revised manuscript.

Furthermore, we showed the result of NMI(θ_S, fPET)/NMI(θ_V, fPET) ratio as a function of vegetation type in Fig. A1. The conclusion that the overall fPET information contained in θ_S is slightly higher than that of θ_V does not vary with vegetation types, although NMI(θ_S, fPET) is much higher than NMI(θ_V, fPET) in open shrubland and woody savannas.

For the rest comments annotated in the manuscript:

1. P6 Line 141. *Ac* and *As* not defined

We've made the following revision in Section 2.2 to clearly defined *Ac* and *As*:

"Based on V_{max}, photosynthesis rates per unit LAI including carboxylase-limited (Rubisco limited, denoted by A_C) type and export-limited (for C3 plants, denoted by A_S) type are calculated respectively."

2. P9 Line 211-215. Maybe a statement to point to section 3.1 is necessary here.

As suggested, we've added a statement to directly point to results starting from Section 3.1:
"Therefore, relative comparisons between NMI(θ_S, fPET) and NMI(θ_V, fPET) are based on examining the size of their mutual ratio NMI(θ_S, fPET)/NMI (θ_V, fPET)."

3. P9 Line 222. Is it for Case I?
Yes, the "vertically-integrated (0–40 cm) soil moisture" is estimated from Case I. We've also clarified this in Section 3.1:
"…i.e., the relative magnitude of fPET information contained in surface soil water content and vertically-integrated (0–40 cm) soil water content estimated from Case I…"

4. P14 Line 287. Even though the sample size is small it would be nice to have also similar plots and the plots above for different vegetation type.
As suggested, we've revised Fig. 4 so that samples are plotted separately according to their vegetation types. With varying magnitudes, the overall overestimation of GLEAM is observed across different vegetation types.

5. P14 Line 291-294. This trend is not really evident. I see an evident increasing ratio only when AI approaches to zero. Maybe a statistical significance of this trend should analyzed.
As suggested, we've added analysis of statistical significance of this trend. Indeed, the increasing trend of NMI(θ_S, fPET)/NMI(θ_V, fPET) ratio is more evident for CLSM, with a moderate goodness-of-fit (0.28). We've also clarified this in Section 3.4:
"With increasing AI, there is a significant decreasing trend in both NMI(θ_S, fPET) and NMI(θ_V, fPET) for all three simulations, with a goodness-of-fit above 0.5 (figure not shown). For all cases, the NMI(θ_S, fPET)/NMI(θ_V, fPET) ratios are consistently greater than unity under all climatic conditions. However, the estimated NMI(θ_S, fPET)/NMI(θ_V, fPET) ratios from all three simulations (NOAHMP, CLSM and GLEAM) exhibit quite different trends with respect to AI. The NMI(θ_S, fPET)/NMI(θ_V, fPET) ratio for CLSM decreases with increasing AI, with a moderate goodness-of-fit value of 0.28,…"

6. P15 Line 315. This can also depend upon the vegetation type as grass and trees are characterized by different root depths. They can exert a different effects on the coupling between soil moisture and evapotranspiration.
Thanks for the comments. This concern of different root depths impact is addressed by applying different methods to retrieve vertically integrated θ as we stated in Section 2.1. The entire analysis is based on the default case I that exponentially filter θ to a unified 40 cm bottom layer depth, and it is found that the overall fPET information contained in θ_S is slightly higher than that of θ_V. However, the difference between NMI(θ_S, fPET) and NMI(θ_V, fPET) is less obvious when using different methods for calculating θ_V using AmeriFlux observations.

In addition, we've showed the result of NMI(θ_S, fPET)/NMI(θ_V, fPET) ratio as a function of vegetation type in Fig. A1. The conclusion that the overall fPET information

contained in θ_S is slightly higher than that of θ_V does not vary with vegetation types, although NMI(θ_S, fPET) is obviously higher than NMI(θ_V, fPET) in open shrubland and woody savannas.

Reply to Referee #2 interactive comment

We would like to thank Referee #2 for the constructive comments.

This is a well written paper with a clear contribution to ecohydrological modeling and I have very few comments. The first relates to the jargon in the title. Please try to simplify the title for the paper to be appealing to a wider audience. Secondly, the aims and objectives of the paper must be clearly formulated and also indicate what is new or novel about this study and who benefits from it? Lastly, what is the take-home message from this study given that no conclusions are given?
Thanks for the comments. We agree that our original title could be improved. Accordingly, the title of revised manuscript has been changed to "Model Representation of the Coupling between Evapotranspiration and Soil Water Content at Different Depths." We feel that this is more accessible to a broader audience.

In addition, we've revised the abstract and introduction to better emphasize the aim and objectives of the paper and provide a concise summary of major conclusion and the target readers with most potential interest are also highlighted in the abstract.

SPECIFIC COMMENTS
- Keywords: - "surface evapotranspiration" is listed as a keyword/phrase. Delete the word "surface"
Thank you for these comments. The keyword of "surface evapotranspiration" has been revised as suggested.

- Line 27 – indicate that some if the incoming energy is absorbed by the surface… given that you are mentioning biochemical cycles in line 30
To avoid this issue, we've removed all mentions of biochemical cycles in the manuscript.

- There are inconsistencies throughout the paper regarding the evaporation terms. A typical example is in lines 11 to 12 in the abstract where the authors refer to the sensible heat flux and evapotranspiration (ET) in the same sentence. Rather also use the energy equivalent of ET (i.e. the latent heat flux) and be consistent throughout the paper.
Thank you for this comment – we agree this was an issue in the original manuscript. In the revised version, the energy equivalent of ET (i.e., the latent heat flux) has been used consistently when also referencing sensible heat flux.

- Line 59: What is meant by ET entropy? This is not a standard micrometeorology or ecohydrological phrase. Please define such terms.
Thank you for the comments. The original expression of "corresponding ET entropy" refers to the entropy of a corresponding ET time series. This is clarified in the revised

manuscript.

- Throughout the paper rather use the phrase “soil water content” which is more specific than “soil moisture”
We’ve replaced the expressions of “soil moisture” with “soil water content” throughout the manuscript.

- Lines 63-64 not necessary
These two unnecessary sentences have been removed as suggested.

- Line 75 sounds rather cyclic, rephrase!
The sentence has been rephrased to “*As described above, θ/ET coupling assessments made using AmeriFlux observations are compared with those using state-of-the-art LSMs including…*”

- How did you account for the accuracy of the different types of soil water content sensors or their depth of installation across the AmeriFlux sites? How does this affect your results?
As the most of the AmeriFlux sites involved in the analysis are using frequency domain reflectometer probe for soil water content measurements, the impact of different sensors on our conclusion is limited.

Secondly, to minimize the effect of different measurement depths on our analysis, we designed three different cases to estimate vertically integrated soil water content (θ_V). Case I was based on the application of an exponential filter (Wagner et al., 1999; Albergel et al., 2008) to extrapolate θ_S to a consistent 40 cm bottom layer depth. Therefore, only θ_S was used to derive θ_V and the bottom-layer (or second layer) AmeriFlux θ measurement was neglected in this case. Nevertheless, since the quality of θ_V estimates is important in our analysis, we also calculated two additional cases where 0–40 cm θ_V was estimated using: 1) the bottom-layer soil water content measurement acquired at each AmeriFlux site (hereinafter, Case II) and 2) linear interpolation of θ_S and the bottom-layer AmeriFlux soil water content measurement (hereinafter, Case III).

The sensitivity of key results show that compared to the baseline Case I of exponential filter extrapolated 40-cm bottom layer θ_V, LSMs and GLEAM agree with AmeriFlux observations in that the overall fPET information contained in θ_S is slightly higher than that of θ_V. However, the sensitivity analysis showed this difference between NMI(θ_S, fPET) and NMI(θ_V, fPET) diminishes when using different methods for calculating θ_V using AmeriFlux observations. These experimental designs and the corresponding findings are clearly stated in the revised manuscript.

- The vegetation acts as the link between the atmosphere and soil water content in deep soil profiles. Please give more details on how the vegetation types affected your

analysis/results.

Thanks for the comments. As mentioned in the response to the previous comment, in order to minimize the effect of different root depths from different vegetation types on NMI(θ_S, fPET) and NMI(θ_V, fPET), we used an exponential filter to extrapolate θ to a unified 40 cm bottom layer depth and find that the overall fPET information contained in θ_S is slightly higher than that of θ_V. However, the difference between NMI(θ_S, fPET) and NMI(θ_V, fPET) diminishes when using different methods for calculating θ_V using AmeriFlux observations.

We've added more extensive discussion regarding the role of vegetation on key results in the revised manuscript. In particular, Fig. 4 has been newly expanded to better isolate the impact of vegetation type and the role of vegetation types is now directly addressed via new text appearing in Section 3.3 of the revised manuscript.

Furthermore, we showed the result of NMI(θ_S, fPET)/NMI(θ_V, fPET) ratio as a function of vegetation type in Fig. A1. The conclusion that the overall fPET information contained in θ_S is slightly higher than that of θ_V does not vary with vegetation types, although NMI(θ_S, fPET) is much higher than NMI(θ_V, fPET) in open shrubland and woody savannas.

- Line 107: What is the bottom layer soil moisture measurement? Define this, else rephrase.

As soil water content measurements are generally available at two discrete depths at the AmeriFlux sites, the bottom layer measurements refer to the measurements at the deeper depth or the second observation layer from surface. This has been clarified in the revised manuscript.

- 2) options for θ factor for stomatal resistance (the β factor). Not clear what this represents. What is a theta factor? What does it do? - and reference soil moisture (m3 m-3), How is this defined? Confusion over symbols.

The θ factor stands for soil water content, and different expressions of θ lead to different representations of relationship between θ and stress factor β. We've revised the original expression to "*…and schemes controlling the effect of θ on the vegetation stress factor β*". As clarified in the revised manuscript, reference soil moisture is set as field capacity in the NOAH users' guide for parameterization.

- Sometimes you mention stomatal resistance, and at other times stomatal conductance; line 142. Choose one and stick to it otherwise this easily gets very confusing.

As suggested, we've revised the only occurrences of the term "stomatal conductance" in Section 2.2 into "stomatal resistance" to avoid any confusion.

- line142 – stomatal conductance is not the sole driver of ET. It's more complex than that.

To avoid such confusion, we've revised expression as "*The minimum of A_C, A_S and*

light-limited photosynthesis rate determines stomatal resistance r_s, and consequently affects ET over vegetated areas".

- Please elaborate - Eqn 6: what does the symbol H mean here? Thought you said H was the sensible heat flux earlier?

In the original Eq. 6, H represents Shannon-type entropy of the variable ζ. Indeed, it could be easily confused with sensible heat flux symbol mentioned in Section 1. Therefore, we've replaced the symbol H in Eq. 6 with SE.

- Fig 4 these are poor model performances.

Indeed, the consistency of NMI(θ, fPET) between models and observations varies across different vegetation types, and varies across different models. However, it should be noted that the absolute value of NMI(θ, fPET) is not a direct index to measure model performance. Furthermore, our analysis conclusion will not be affected as we are using the relative ratio of NMI(θ_S, fPET)/NMI(θ_V, fPET).

~~Land Surface~~ Model Representation of the ~~Mutual Information Context~~ Coupling between ~~Multi-Layer Soil Moisture and~~ Evapotranspiration and Soil Water Content at Different Depths

Jianxiu Qiu[1,2], Wade T. Crow[3], Jianzhi Dong[3], Grey S. Nearing[4]

[1]Guangdong Provincial Key Laboratory of Urbanization and Geo-simulation, School of Geography and Planning, Sun Yat-sen University, Guangzhou, 510275, China

[2]Southern Laboratory of Ocean Science and Engineering (Guangdong, Zhuhai), Zhuhai, 519000, China

[3]USDA ARS Hydrology and Remote Sensing Laboratory, Beltsville, MD 20705, USA

[4]Department of Geological Sciences, University of Alabama, AL 35487, USA

Correspondence to: Jianxiu Qiu (qiujianxiu@mail.sysu.edu.cn)

Abstract. Soil ~~moisture~~water content (θ) ~~impacts~~influences the climate system by ~~regulating~~ controlling fraction of incoming solar and longwave energy that is converted into evapotranspiration (ET)~~into outgoing evapotranspiration (ET) and sensible heat flux components~~. Therefore, investigating the coupling strength between θ and ET is important for the study of land surface/atmosphere interactions. Physical models are commonly tasked with representing the coupling between θ and ET; however, few studies have evaluated the accuracy of model-based estimates of θ/ET coupling (especially at multiple soil depths). To address this issue~~Here~~, we use in-situ AmeriFlux observations to evaluate θ/ET coupling strength estimates acquired from multiple land surface models (LSMs) and an ET retrieval algorithm – the Global Land Evaporation Amsterdam Model (GLEAM). For maximum robustness, coupling strength is represented using the sampled normalized mutual information (NMI) between θ estimates acquired at various vertical depths and surface evaporation flux expressed as a~~represented by~~ fraction of potential evapotranspiration (fPET, the ratio of ET to potential ET). Results indicate that LSMs and GLEAM are generally in agreement with AmeriFlux measurements in that surface soil ~~moisture~~water content (θ_S) contains slightly more NMI with fPET than vertically integrated soil ~~moisture~~water content (θ_V). Overall, LSMs and GLEAM adequately capture variations in NMI between fPET and θ estimates acquired at various vertical depths. However, ~~one model – the Global Land Evaporation Amsterdam Model (~~GLEAM~~) –~~ significantly overestimates the NMI between θ and ET and the relative contribution of θ_S to total ET. This bias appears attributable to differences in GLEAM's ET estimation scheme relative to the other two LSMs considered here (i.e., the Noah model with m~~M~~ulti–parameterization options and the Catchment Land Surface Model). These results provide insight into improved LSM model structure and parameter optimization for land surface-atmosphere coupling analyses.

Keywords. Land surface/atmosphere interaction, soil ~~moisture~~water content, ~~surface~~ evapotranspiration

1 Introduction

Soil ~~moisture~~water content (θ) modulates water and energy feedbacks between the land surface and the lower atmosphere by ~~partitioning incoming energy into evapotranspiration (ET) and sensible heat (H) surface flux components~~determining the fraction of incoming solar energy that is converted in evapotranspiration (ET) (Seneviratne et al., 2010, 2013). In water-limited regimes, θ exhibits a dominant control on ET ~~and~~, and therefore ~~e, commonly~~ exerts significant terrestrial control on the earth's water and~~,~~ energy ~~and biochemical~~ cycles. Accurately representing θ/ET coupling in land surface models (LSMs) is therefore expected to improve our ability to project the future frequency of extreme climates (Seneviratne et al., 2013).

A key question is how the constraint of θ on ET and H varies as θ is vertically integrated over deeper vertical soil depths. Given the tendency for the time scales of θ dynamics to vary strongly with depth, the degree to which the ET is coupled with vertical variations in θ determines the temporal scale at which θ variations are propagated into the lower atmosphere. Therefore, in order to represent θ/ET coupling, and thus land/atmosphere interactions in general, LSMs must accurately capture the relationship between vertically varying θ values and ET. Unfortunately, their ability~~ies~~ to do so remains an open question.

Recently, land surface/atmosphere coupling strength has been investigated by sampling mutual information proxies (e.g., correlation coefficient or other coupling indices) between time series of θ and ET observations (or air temperature proxies for ET). Results suggest that, even when confined to very limited vertical support (e.g., within the top 5 cm of the soil column), surface θ estimates retain significant information for describing overall~~examining~~ θ control~~s~~ on local climate (Ford and Quiring, 2014b; Qiu et al., 2014; Dong and Crow, 2018; Dong and Crow, 2019). These findings are in contrast with the common perception~~s~~ that ET is constrained only~~dominated~~ by θ values within~~at~~ deeper soil layers (Hirschi et al., 2014). Hence, it is necessary to examine whether LSMs can realistically reflect observed variations of θ/ET coupling strength ~~in the~~within the vertical soil profile~~s~~.

Previous studies examining the θ/ET relationship have generally been based on Pearson product-moment correlation (Basara and Crawford, 2002; Ford et al., 2014a), which captures only the strength of a linear relationship between two variables. However, the coupling between θ and ET is generally nonlinear. Therefore, non-parametric mutual information measures are generally more appropriate. Nearing et al. (2018) used information theory metrics (transfer entropy, in -particular) to measure the strength~~s~~ of direct~~ed~~ couplings between different surface variables, including soil ~~moisture~~water content, and surface energy fluxes at short timescales in several LSMs. They found that the LSMs are~~were~~ generally biased as compared with strengths of couplings in observation data, and that these biases differ~~ed~~ across different study sites. However, they did not look specifically at the effect of vertical ~~moisture~~water content profiles or of subsurface soil ~~moisture~~water content on partitioning surface energy fluxes.

Here we apply the information theory-based methodology of Qiu et al. (2016) to examine the relationship between the vertical support of θ estimates and their mutual information (MI) with respect to ET. Our approach is based on analyzing the MI content between ET and θ time series - acquired from both LSMs, ET retrieval algorithm – the Global Land Evaporation Amsterdam Model (GLEAM) and AmeriFlux in-situ observations. MI values are then normalized by entropy in the corresponding ET time series ~~corresponding ET entropy~~ to remove the effect of inter-site variations to~~and~~ generate estimates of Normalized Mutual Information (NMI) between θ and ET. ~~Examined θ time series have two different vertical supports:~~ Both surface (roughly 0–10 cm) soil ~~moisture~~water content (θ_S) and vertically integrated (0–40 cm) soil ~~moisture~~water content (θ_V) are considered to capture the impact of depth on NMI results. AmeriFlux-based -NMI results are then compared with analogous NMI results obtained from LSM-based and GLEAM-based θ and ET time series.

~~Further details on our methodology are presented in Sect. 2. Results are presented in Sect. 3 and discussed/summarized in Sect. 4.~~

2 Data and Methods

The AmeriFlux network provides temporally continuous measurements of θ, surface energy fluxes and related environmental variables for sites located in a variety of North American ecosystem types, e.g., forests, grasslands, croplands, shrublands and savannas (Boden, et al., 2013). To minimize sampling errors, AmeriFlux sites lacking a

complete 3-year summer months (June, July and August) daily time series between the years of 2003 and 2015 (i.e., 3×92=276 daily observations in total) of θ_S, θ_V and latent heat flux (LE) are~~were~~ excluded here - resulting in the 34 remaining eligible AmeriFlux sites listed in Table 1. These sites cover a variety of climate zones within the contiguous United States (CONUS). Table 1 gives background information on these 34 sites including local land cover information. Hydro-climatic conditions in each site are~~were~~ characterized using the aridity index (AI) – calculated using CRU (Climate Research Unit, v4.02) monthly precipitation and potential evaporation (PET) datasets.

As described above, θ/ET coupling assessments made using AmeriFlux observations are~~were~~ compared with ~~comparable assessments based on output from~~those using state-of-the-art LSMs including the Noah model with ~~M~~multi–parameterization options (NOAHMP) and ~~,~~ Catchment Land Surface Model (CLSM). In addition, ~~and~~ θ and ET retrievals provided by the Global Land Evaporation Amsterdam Model (GLEAM) are also considered. See below for~~r more model~~ details on all three approaches. To avoid any spurious correlations between θ and ET due to seasonality, all NMI analyses are~~were~~ performed on θ and ET time series anomalies acquired during the period 2003–2015. The θ and ET anomalies are~~were~~ calculated by removing the seasonal cycle – defined as 31-day window averages centered on each day-of-year sampled across all years of the 2003–2015 historical data record – from the raw θ and ET time series data. The analysis ~~was~~ is limited to the CONUS during summer months (June, July and August) when θ/ET coupling i~~was~~ expected to be maximized.

Table 1 Attributes of selected AmeriFlux sites

AmeriFlux sites	Land cover	Elevation [m]	Top-layer depth [cm]	Bottom-layer depth [cm]
ARM SGP Main	Cropland	314	10[a]	20[b]
ARM USDA UNL OSU Woodward Switchgrass 1	Grassland	611	10	30
Audubon Research Ranch	Grassland	1469	10	20
Bondville	Cropland	219	10[c]	20
Brookings	Grassland	510	10	20
Chimney Park	Evergreen needleleaf forest	2750	0-15	15-45
Duke Forest Hardwoods	Deciduous broadleaf forest	168	10	25
Duke Forest Open Field	Grassland	168	10	25
Fermi Agricultural	Cropland	225	2.5	10
Fermi Prairie	Grassland	226	2.5	10
Flagstaff Managed Forest	Evergreen needleleaf forest	2160	2	10
Flagstaff Unmanaged Forest	Woody savannas	2180	2	10
Flagstaff Wildfire	Grassland	2270	2	10
Fort Peck	Grassland	634	5[d]	20
Freeman Ranch Woodland	Woody savannas	232	10	20
Glacier Lakes Ecosystem Experiments Site	Evergreen needleleaf forest	3190	5	10
Howland Forest Main	Mixed forest	60	NA	NA

Lucky Hills Shrubland	Open shrubland	1372	5	15
Marys River Fir Site	Evergreen needleleaf forest	263	10	20
Metolius Intermediate Pine	Evergreen needleleaf forest	1253	0-30	NA
Missouri Ozark	Deciduous broadleaf forest	219	10	100
Nebraska SandHills Dry Valley	Grassland	1081	10	25
Quebec Boreal Cutover Site	Evergreen needleleaf forest	400	5	20
Quebec Mature Boreal Forest Site	Evergreen needleleaf forest	400	5	10
Santa Rita Creosote	Open shrubland	991	2.5	12.5
Santa Rita Mesquite	Woody savannas	1116	2.5-5	5-10
Sherman Island	Grassland	-5	10	20
Sylvania Wilderness	Mixed forest	540	5	10
Tonzi Ranch	Woody savannas	169	0	20
University of Michigan Biological Station	Deciduous broadleaf forest	234	0-30	NA
Vaira Ranch	Grassland	129	0	10
Walker Branch	Deciduous broadleaf forest	343	5	10
Willow Creek	Deciduous broadleaf forest	515	5	10
Wind River Field Station	Evergreen needleleaf forest	371	30[e]	50[f]

[a] Was 5 cm prior to 4/13/2005
[b] Was 25 cm prior to 4/13/2005
[c] Was 5 cm prior to 1/1/2006
[d] Was 10 cm (2003-2008)
[e] Was 0-30 cm prior to 2007
[f] ~~Was NaN~~Unavailable ~~-~~prior to 2007

2.1 Ground-based AmeriFlux measurements

The Level 2 (L2) AmeriFlux LE and sensible heat (H) flux observations are based on high-frequency (typically > 10 Hz) eddy covariance measurements processed into half-hourly averages by individual AmeriFlux investigators. LE and θ observations at a half-hour time step and without gap-filling procedures are~~were~~ collected from the AmeriFlux Site and Data Exploration System (see http://ameriflux.ornl.gov/). The LE and θ observations are~~were~~ further aggregated into daily (0 to 24 UTC) values, and daily LE i~~was~~s converted into daily ET using the latent heat of vaporization. Daily ET values based on less than 30% half-hourly coverage (i.e., < 15 half-hourly observations per day) are~~were~~ considered not representative at a daily time scale and therefore excluded.

Soil ~~moisture~~water content measurements are generally available at two discrete depths that vary between the AmeriFlux sites (Table 1). Here, the top (i.e., closest to the surface) soil ~~moisture~~water content observation i~~was~~s always used to represent surface soil ~~moisture~~water content (θ_S). Since the depth of this top~~-~~-layer measurement varies between 0 and 15 cm (see Table 1), we consider the surface-layer measurement θ_S to be roughly representative of 0–10 cm (vertically integrated) θ.

Given variations in the depth of the lower AmeriFlux θ observations (see Table 1), we applied a variety of approaches for estimating vertically integrated soil ~~moisture~~water content (θ_V). Our first approach, hereinafter referred to as Case

I, iwas based on the application of an exponential filter (Wagner et al., 1999; Albergel et al., 2008) to extrapolate θ_S to a consistent 40–cm bottom layer depth. Therefore, only θ_S iwas used to derive θ_V and the bottom-layer (or second layer) AmeriFlux θ measurement iwas neglected in this case. The application of the exponential filter requires a single time-scale parameter T. Since θ measurements from United States Department of Agriculture's Soil Climate Analysis Network (SCAN) are taken at fixed soil depth, we utilized this dataset to determine the most appropriate parameter T at AmeriFlux sites. Following Qiu et al. (2014), first, we estimated the optimal parameter T (Topt) for the extrapolation of θ measurements from 10 cm to 40 cm depth and established a global relationship between Topt and site-based NDVI (MOD13Q1 v006, 250m, 16-day) (Topt = 2.098 × exp(–1.895 × (NDVI + 0.6271)) + 2.766). Then, this global relationship (Goodness of Fit R^2: 0.85) was is applied to AmeriFlux sites to extrapolate 0–10 cm θ_S times series into 0–40 cm θ_V.

Previous research has suggested that such a filtering approach does not significantly squander ET information present in actual measurements of θ_V (Qiu et al., 2014; Qiu et al., 2016). Nevertheless, since the quality of θ_V estimates is important in our analysis, we also calculated two additional cases where 0–40 cm θ_V iwas estimated using: 1) the bottom-layer soil moisturewater content measurement acquired at each AmeriFlux site (hereinafter, Case II) and 2) linear interpolation of θ_S and the bottom-layer AmeriFlux soil moisturewater content measurement (hereinafter, Case III). The sensitivity of key results to these various cases is discussed below.

2.2 LSM-based and GLEAM-based simulations

LSM outputSimulations iwas acquired from NOAHMP (Niu et al., 2011) and CLSM (Koster et al., 2000) LSMs simulations embedded within the NASA Land Information System (LIS, Kumar et al., 2006) and the GLEAM a ET retrieval algorithmsatellite observation based model GLEAM (Miralles et al., 2011). Both NOAHMP and CLSM arewere set-up to simulate 0.125 ° θ profiles at a 15-minute time step using North America Land Data Assimilation System, Phase 2 (NLDAS-2) forcing data. A 10-year model spin-up period (1992 to 2002) iwas applied for NOAHMP and CLSM.

NOAHMP numerically solves the one-dimensional Richards equation within four soil layers of thicknesses of 10, 30, 60, and 100 cm. Major parameterization options relevant to θ simulation include : 1) options for canopy stomatal resistance parameterization; 2) options for and schemes controlling the effect of θ on the vegetation stress factor $\beta\theta$ factor for stomatal resistance (the β factor). Here we employed the Ball-Berry-type stomatal resistance scheme and Noah-type soil moisturewater content factor controlling the β factor. The specific expressions are as follows:

$$\beta = \sum_{i=1}^{N_{\text{root}}} \frac{\Delta Z_i}{Z_{root}} \min\left(1.0, \frac{\theta_i - \theta_{\text{wilt}}}{\theta_{\text{ref}} - \theta_{\text{wilt}}}\right) \quad (1)$$

where θ_{wilt} and θ_{ref} are respectively soil moisturewater content at witling point (m^3 m^{-3}) and reference soil moisturewater content (m^3 m^{-3}), which is close to set as field capacity during parameterization. θ_i and Δz_i are soil

~~moisture~~water content ($m^3\ m^{-3}$) and soil depth (cm) at *i*th layer, N_{root} and z_{root} are total number of soil layers with roots and total depth (cm) of root zone, respectively.

Following the Ball-Berry stomatal resistance scheme, the θ-controlled β factor and other multiplicative factors including temperature, foliage nitrogen simultaneously determine the maximum carboxylation rate V_{max} as follows:

$$V_{\max} = V_{\max 25}\, \alpha_{\mathrm{vmax}}^{\frac{T_{\mathrm{v}}-25}{10}}\, f(N) f(T_{\mathrm{v}})\, \beta \tag{2}$$

where V_{max25} is maximum carboxylation rate at 25 ℃ (μmol CO_2 m^{-2} s^{-1}); α_{vmax} is a parameter sensitive to vegetation canopy surface temperature T_v; $f(N)$ is a factor representing foliage nitrogen and $f(T_v)$ is a function that mimics thermal breakdown of metabolic processes. Based on V_{max}, ~~carboxylase-limited (Rubisco-limited) and export-limited (for C3 plants)~~ photosynthesis rates per unit LAI including carboxylase-limited (Rubisco limited, denoted by A_C) type and export-limited (for C3 plants, denoted by A_S) type~~(A_C and A_S respectively)~~ are calculated respectively.~~, and the~~ The minimum of A_C, A_S and light-limited photosynthesis rate~~s~~ determine~~s~~ stomatal resistance~~conductance~~ r_s, and~~,~~ consequently affects~~the~~ ET over vegetated areas. For the complete NOAHMP configuration, please see Table S1 in the supplementary material.

CLSM simulates the 0–2 and 0–100 cm soil ~~moisture~~water content and evaporative stress as a function of simulated θ and environmental variables. ET is then estimated based on the estimated evaporative stress and land-atmosphere humidity gradients. Energy and water flux estimates are iterated with soil state estimates (e.g., θ and soil temperature) to ensure closure of surface energy and water balances. For a~~the~~ detailed explanation of CLSM physics, please refer to Koster et al. (2000).

GLEAM is a set of algorithms dedicated to the estimation of terrestrial ET and root-zone θ from satellite data. In this study, the latest version of this model (v3.2a) is employed. In GLEAM, the configuration of soil layers varies as a function of the land-cover type. Soil stratification is based on three soil layers for tall vegetation (0–10, 10–100, and 100–250 cm), two layers for low vegetation (0–10, 10–100 cm) and only one layer for bare soil (0–10 cm) (Martens et al., 2017).

The cover-dependent PET (mm day^{-1}) of GLEAM is calculated using the Priestley and Taylor (1972) equation based on observed air temperature and net radiation. Following this, estimates of PET are~~were~~ converted into actual transpiration or bare soil evaporation (depending on the land-cover type, ET (mm day^{-1})), using a cover-dependent, multiplicative stress factor S (–), which is calculated as a function of microwave vegetation optical depth (VOD) and root-zone θ (Miralles et al., 2011). The related expressions are as follows:

$$\mathrm{ET} = \mathrm{PET} \times S + E_{\mathrm{i}} \tag{3}$$

$$S = \sqrt{\frac{\mathrm{VOD}}{\mathrm{VOD}_{\max}}} \left(1 - \left(\frac{\theta_{\mathrm{c}} - \theta\omega}{\theta_{\mathrm{c}} - \theta_{\mathrm{wilt}}}\right)^2\right) \tag{4}$$

where E_i is rainfall interception (mm); S essentially represents the fPET (see Sect. 2.3) estimated by GLEAM; θ_c (m^3 m^{-3}) is the critical soil ~~moisture~~water content and θ_ω (m^3 m^{-3}) is the soil ~~moisture~~water content of the wettest layer, assuming that plants withdraw water from the layer that is most accessible. Based on (4), GLEAM S (or fPET) tend to become more sensitive to θ in areas of low VOD seasonality (i.e., low differences between VOD and VOD_{max}). As for bare soil conditions, S is linearly related to surface soil ~~moisture~~water content (θ_1):

$$S = 1 - \frac{\theta_c - \theta_1}{\theta_c - \theta_{wilt}}. \quad (5)$$

To resolve variations in the vertical discretization of θ applied by each model, we linearly interpolated NOAHMP, CLSM and GLEAM outputs into daily 0–10 and 0–40 cm soil ~~moisture~~water content values using depth-weighted averaging.

2.3 Variable indicating soil ~~moisture~~water content and surface flux coupling

Soil ~~moisture~~water content – ET coupling can be diagnosed using a variety of different variables derived from ET, e.g. the fraction of PET (fPET, the ratio of ET and PET) or the evaporative fraction (EF, the ratio of LE and the sum of LE and sensible heat). Since ET is strongly tied to net radiation (Rn) (Koster et al., 2009), both fPET and EF are advantageous in that they normalize ET by~~and~~ removing the impact of non-soil ~~moisture~~water content influences on ET (e.g., net radiation, wind speed and soil heat flux (G)). However, since sensible heat flux is not provided in the GLEAM dataset, we are restricted here to using fPET.

It should be noted that the applied meteorological forcing data for NOAHMP and CLSM are~~were~~ somewhat different from those used for GLEAM. Therefore, to minimize the impact of this difference, NOAHMP and CLSM fPET ~~were~~ are computed from North American Regional Reanalysis (NARR) using the modified Penman scheme of Mahrt and Ek (1984) while GLEAM fPET i~~wa~~s calculated using its own internal PET estimates. To examine the impact of PET source on results, AmeriFlux fPET calculations are~~were~~ ~~calculated~~ duplicated using both GLEAM- and NARR-based PET values.

2.4 Information measures

Mutual information (MI) (Cover and Thomas, 1991) is a nonparametric measure of correlation between two random variables. MI and the related Shannon-type entropy (SE, Shannon, 1948) are calculated as follows. Entropy about a random variable ζ is a measure of uncertainty according to its distribution p_ζ and is estimated as the expected amount of information from p_ζ sample:

$$SE~~H~~(p_\zeta) = E_\zeta[-\ln(p_\zeta(\zeta))]. \quad (6)$$

Likewise, MI between ζ and another variable ψ can be thought of as the expected amount of information about variable ζ contained in a realization of ψ and is measured by the expected Kullback-Leibler (KL) divergence (Kullback and Leibler, 1951) between the conditional and marginal distributions over ζ:

$$\mathrm{MI}(\zeta;\psi) = \mathrm{E}\psi[D(p_{\zeta|\psi} \parallel p_{\zeta})]. \quad (7)$$

In this context, the generic random variables ζ and ψ represent fPET and θ (soil ~~moisture~~water content) respectively. The observation space of the target random variable fPET i~~wa~~s discretized using a fixed bin width. As bin width decreases, entropy increases but mutual information asymptotes to a constant value. On the other hand, increased bin width requires more sample size, which cannot always be satisfied. The trick is choosing a bin width where the NMI values stabilize with sample size. After a careful sensitivity analysis, we choose a fixed bin width of 0.25 [-] for fPET and make sure that each AmeriFlux site have enough samples to accurately estimate the NMI, and change of this constant bin width from 0.1–0.5 [-] will not significantly alter our conclusions. Following Nearing et al. (2016), a bin width of 0.01 $m^3\ m^{-3}$ (1% volumetric water content) for θ i~~wa~~s applied. Integrations required for MI calculation in Eq. (7) are then approximated as summations over the empirical probability distribution function bins (Paninski, 2003).

By definition, the MI between two variables represents the amount of entropy (uncertainty) in either of the two variables that can be reduced by knowing the other. Therefore, the MI normalized by the entropy of the AmeriFlux-based fPET measurements represents the fraction of uncertainty in fPET that is resolvable given knowledge of the soil ~~moisture~~water content state (Nearing et al., 2013). Unlike Pearson's correlation coefficient, MI is insensitive to the impact of nonlinear variable transformations. Therefore, it is well suited to describe the strength of the (potentially non-linear) relationship between θ and fPET.

Here, we applied this approach to calculate the MI content between soil ~~moisture~~water content representing different vertical depths (as reflected by θ_S and θ_V) and fPET at each AmeriFlux site. All estimated site-specific MI ~~were~~ are normalized by the entropy of the corresponding AmeriFlux-based fPET measurements to remove the effect of inter-site entropy variations on the magnitude of NMI differences. The resulting normalized MI calculations between both θ_S and θ_V and fPET are denoted as NMI(θ_S, fPET) and NMI(θ_V, fPET) respectively.

The underestimation of observed θ/ET coupling via the impact of mutually-independent θ and ET errors in AmeriFlux observations (Crow et al. 2015) i~~wa~~s minimized by focusing on the ratio between NMI(θ_S, fPET) and NMI (θ_V, fPET). Therefore, relative comparisons between NMI(θ_S, fPET) and NMI(θ_V, fPET) are based on examining the size of their mutual ratio NMI(θ_S, fPET)/NMI (θ_V, fPET). To quantify the standard error of NMI differences between various soil ~~moisture~~water content products, we applied a nonparametric, 500-member bootstrapping approach~~,~~ and calculated pooled average of sampling errors across all sites assuming spatially independent sampling error.

Finally, we also examined the impact of potential nonlinearity in the θ/ET relationship by comparing non-parametric NMI results with comparable inferences based on a conventional Pearson's correlation calculation. The correlation-based coupling strength between θ_S and fPET ~~was~~ is denoted as $R(\theta_S$, fPET) and between θ_V and fPET as $R(\theta_V$, fPET).

3 Results

3.1 Comparison of NMI(θ_S, fPET) and NMI(θ_V, fPET)

Figure 1 contains boxplots of modelled and observed NMI(θ_S, fPET) and NMI(θ_V, fPET), i.e., the relative magnitude of fPET information contained in surface soil ~~moisture~~water content and vertically-integrated (0–40 cm) soil ~~moisture~~water content estimated from case I, sampled across all the AmeriFlux locations listed in Table 1. According to the AmeriFlux ground measurements, median values of NMI(θ_S, fPET) and NMI(θ_V, fPET) (across all sites) are near 0.3 [-]. This suggests that approximately 30% of the uncertainty (i.e., entropy at this particular bin width of 0.25 [-]) in fPET can be eliminated given knowledge of either surface or vertically integrated soil ~~moisture~~water content state. This is consistent with earlier results in Qiu et al., (2016) who used similar ~~variables~~ metrics to evaluate θ/EF (evaporative fraction) coupling strength. The sampled medians of NMI(θ_S, fPET) and NMI(θ_V, fPET) estimated by the NOAHMP and CLSM models are similar to these (observation-based) AmeriFlux values. With the single exception that the CLSM predicts much larger site-to-site variation in NMI(θ_S, fPET).

In contrast, NMI(θ_S, fPET) and NMI(θ_V, fPET) values sampled from GLEAM θ and fPET estimates are biased high (with median NMI(θ_S, fPET) and NMI(θ_V, fPET) values of about 0.5 and 0.4 [-], respectively) with respect to all other estimates.

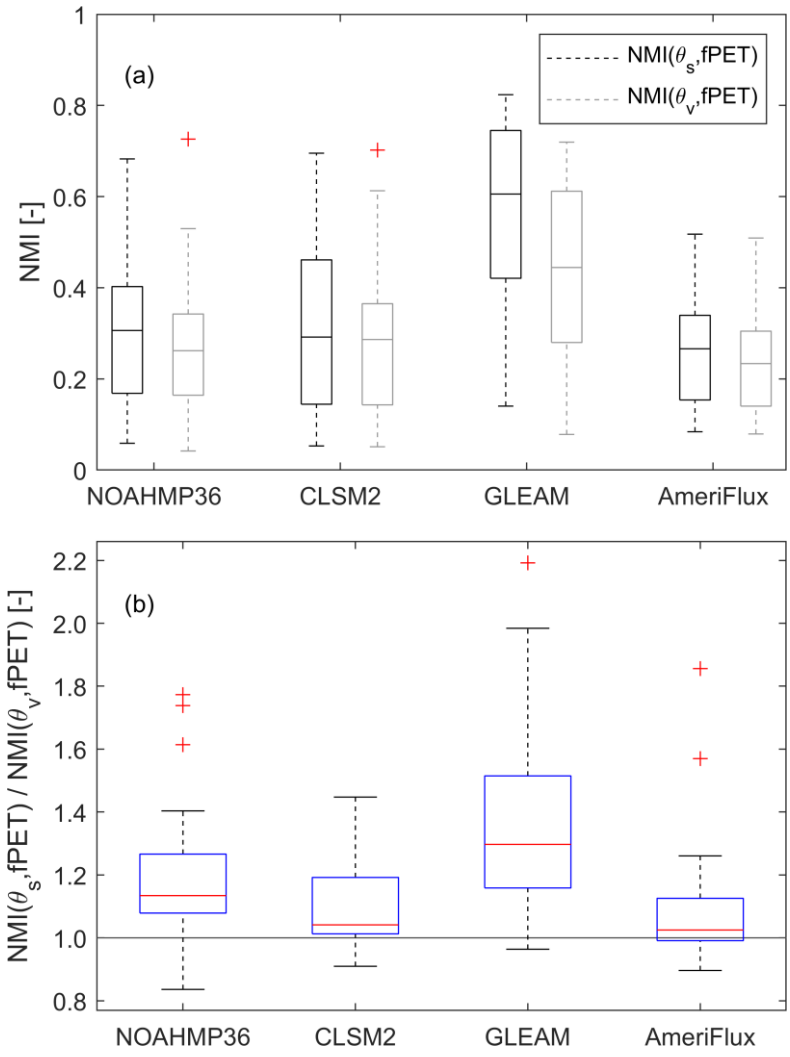

Fig.1 The θ/ET coupling strengths for summertime anomaly time series acquired from various LSMs, GLEAM and AmeriFlux measurements: (a) NMI(θ_S, fPET) and NMI(θ_V, fPET) individually and (b) NMI(θ_S, fPET) normalized by NMI(θ_V, fPET).

~~All three~~Both LSMs and GLEAM overall exhibit significantly (at p = 0.05 [-] confidence, using the 34 AmeriFlux site-collocated samples pixels for pair t-test) higher NMI(θ_S, fPET) compared to NMI(θ_V, fPET) – implying the surface soil ~~moisture~~water content observations contain more fPET information than vertically-integrated soil ~~moisture~~water content observations. However, the observed difference between NMI(θ_S, fPET) and NMI(θ_V, fPET) is less discernible in AmeriFlux measurements (Fig. 1(a)).

Here, AmeriFlux observations are used as a baseline for LSM and GLEAM evaluation. However, it should be stressed that random observation errors in θ and fPET will introduce a low bias into AmeriFlux-based estimates of both NMI(θ_S, fPET) and NMI(θ_V, fPET) (Crow et al., 2015) and thus their difference as well. To address this concern, Fig. 1(b) plots the ratio of NMI(θ_S, fPET) and NMI(θ_V, fPET), which effectively normalizes (and therefore minimizes) the impact of random observation errors~~such observation error impacts~~. As discussed above, these r~~R~~atio results illustrate the general tendency for NMI(θ_S, fPET) > NMI(θ_V, fPET) ~~discussed above~~. They also highlight the tendency for

GLEAM to overvalue θ_S (relative to θ_V) when estimating fPET. A second approach for reducing the random error of θ and fPET measurement errors is the Triple Collocation (TC)-based correction applied in Crow et al. (2015). However, this approach is currently restricted to linear correlation and cannot be applied to estimate NMI. Future work will examine extending the information-based TC approach of Nearing et al. (2017)~~,~~ to the examination of NMI.

3.2 Sensitivity of AmeriFlux-based NMI(θ_S, fPET)/NMI(θ_V, fPET)

As mentioned in Sect. 2.1, an important concern is the impact of interpolation errors used to estimate 0–40 cm θ_V from AmeriFlux θ_S observations acquired at non-uniform depths. To ensure that different methods for calculating AmeriFlux θ_V values do not affect the main conclusion of this study, we configured three cases for θ_V calculation, and compared their NMI(θ_S, fPET)/NMI(θ_V, fPET) results in Fig. 2. Case I reflects the baseline use of the exponential filter described in Sect. 2.1. However, slight changes to AmeriFlux results are noted if alternative approaches are used. Specifically, AmeriFlux-based NMI(θ_V, fPET) increases and closes the gap with NMI(θ_S, fPET) if the bottom-layer soil ~~moisture~~water content measurements are instead directly used as θ_V (Case II) or if 0–40 cm θ_V is based on the linear interpolation of the two AmeriFlux θ observations (Case III), the impact of this modest sensitivity on key results is discussed below.

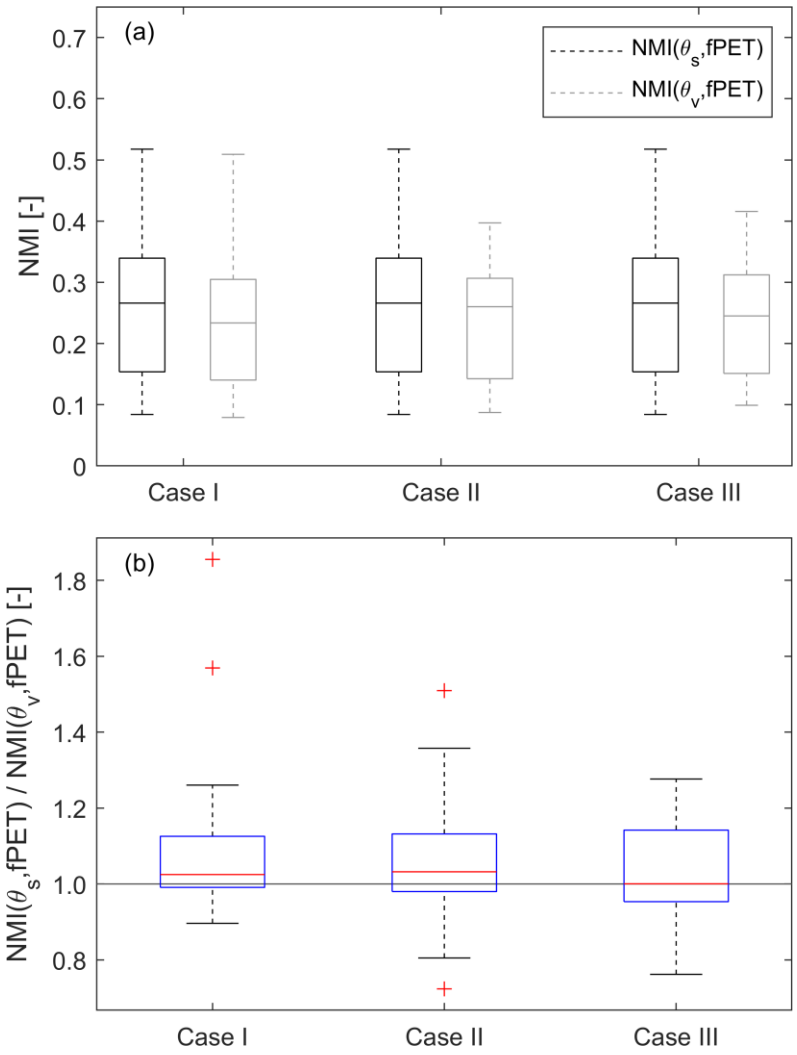

Fig.2 The θ/ET coupling strengths for summertime anomaly time series from AmeriFlux measurements using three different θ_V calculation methods: (a) NMI(θ_S, fPET) and NMI(θ_V, fPET) individually and (b) NMI(θ_S, fPET) divided by NMI(θ_V, fPET) for multiple θ_V cases. Case I is based on the application of an exponential filter to extrapolate 0–10 cm θ_S to a consistent 0–40 cm bottom layer depth, while Cases II and III refer to the direct use of only the bottom layer measurement and a linear interpolation of both the top and bottom layer, respectively, to calculate θ_V (see Sect. 2.1 for details on each case).

In addition, switching from GLEAM- to NARR-based PET when calculating fPET for AmeriFlux-based NMI(θ_S, fPET) and NMI(θ_V, fPET) does not qualitatively change results and produces only a very slight (~6%) increase in the median NMI(θ_S, fPET)/NMI(θ_V, fPET) ratio.

3.3 Spatial distribution of NMI(θ_S, fPET) and NMI(θ_V, fPET)

Figure 3 plots the spatial distribution of NMI(θ_S, fPET) and NMI(θ_V, fPET) results for each of the individual 34 AmeriFlux sites listed in Table 1. The climatic regime is represented by AI (aridity index) values plotted as the background color in Fig. 3. It can be seen in Fig. 3 that NMI(θ_S, fPET) estimates from LSMs and GLEAM are spatially related to hydro-climatic conditions, as NOAHMP and CLSM predict that θ_S is moderately coupled with fPET (i.e., NMI(θ_S, fPET) of 0.3–0.5 [-]) in the arid ~~s~~Southwestern US (AI<0.2) and only loosely coupled with fPET in the

relatively humid eEastern US. A similar decreasing trend of NMI(θ_S, fPET) from the sSouthwestern to eEastern US is also captured by GLEAM. However, as noted above, GLEAM generally overestimates NMI(θ_S, fPET) and NMI(θ_V, fPET) compared to NOAHMP, CLSM and AmeriFlux. In contrast, a relatively weaker spatial pattern emerges in AmeriFlux-based NMI(θ_S, fPET) results. In addition, spatial patterns for NMI(θ_S, fPET) are less defined than for NMI(θ_V, fPET) in all four datasets.

Scatterplots in Fig. 4 summarize the spatial relationship between LSM- and GLEAM-based NMI(θ_S, fPET) and NMI(θ_V, fPET) results versus AmeriFlux observations across different land use types. While observed levels of correlation in Fig. 4 are relatively modest, there ~~appears to be a~~is a significant level (p<0.05) of spatial correspondence between LSMs modelled and observed NMI results only over forest sites – motivating the need to better understand processes responsible for spatial variations in NMI results. In addition, stratifying NMI(θ_S, fPET)/NMI(θ_V, fPET) ratio results according to vegetation type (Fig. A1) confirms that NMI(θ_S, fPET) slightly exceeds NMI(θ_V, fPET) across all vegetation types (and thus all rooting depths characterizing each vegetation type). This suggests that our analysis is not severely affected by variations in the depth of θ measurements. For further discussion on the impact of land cover on NMI results, please see Appendix A.

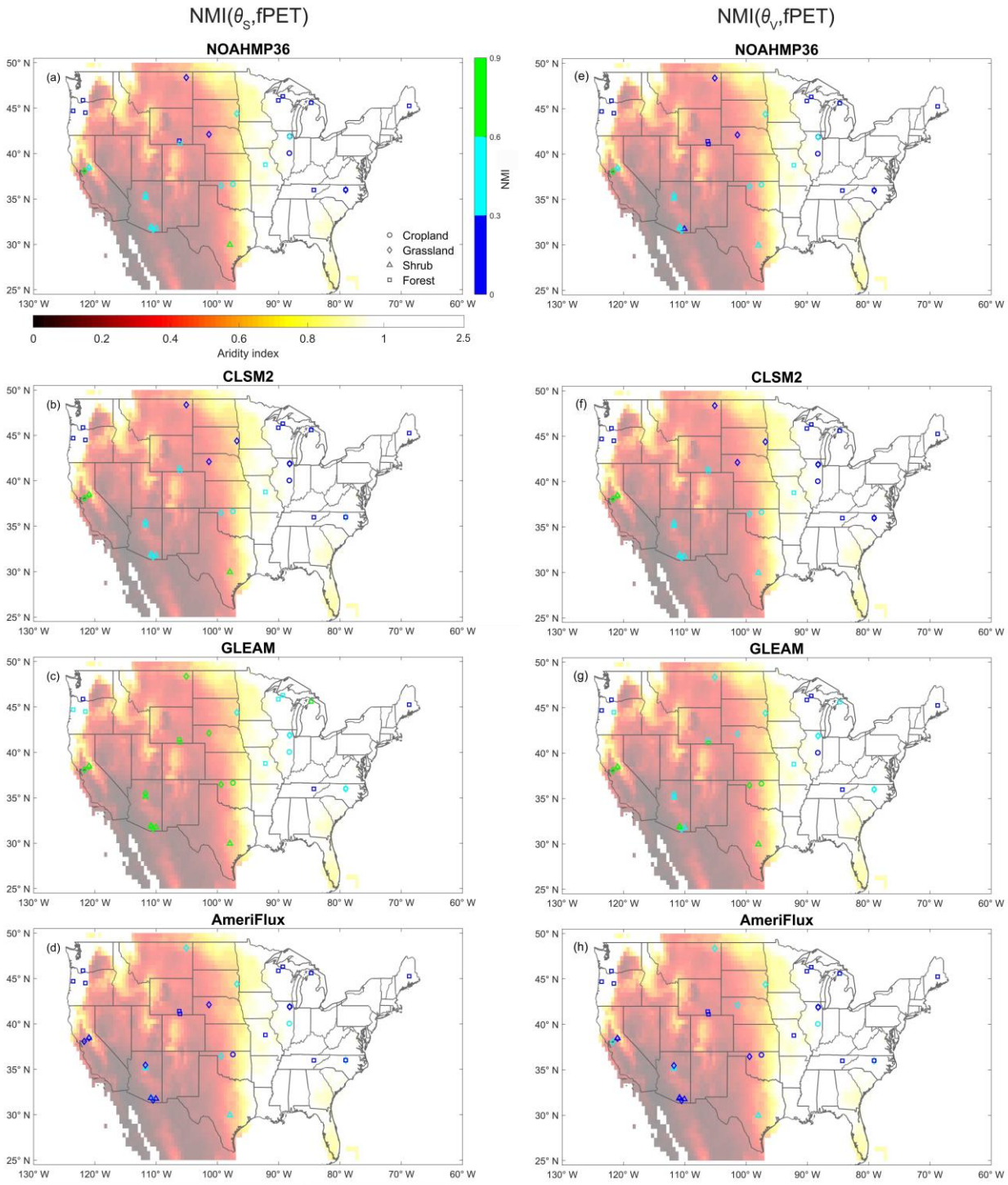

311

312 Fig. 3 NMI(θS, fPET) (left column) and NMI(θV, fPET) (right column) estimates at AmeriFlux sites for: (a) NOAHMP, (b) CLSM,
313 (c) GLEAM and (d) AmeriFlux. Marker color reflects NMI magnitudes and symbol type reflects local land cover type at each site.
314 Background color shading reflects aridity index (AI) values.

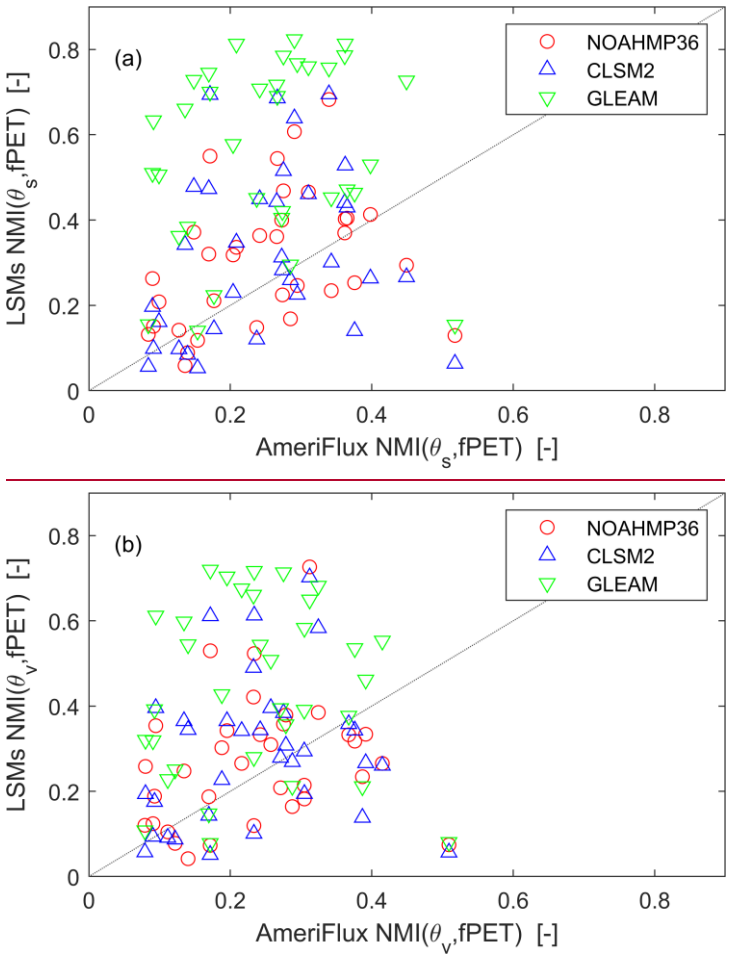
(a)
NOAHMP36
CLSM2
GLEAM
LSMs NMI(θ_s,fPET) [-]
AmeriFlux NMI(θ_s,fPET) [-]
0
0.2
0.4
0.6
0.8
(b)
NOAHMP36
CLSM2
GLEAM
LSMs NMI(θ_v,fPET) [-]
AmeriFlux NMI(θ_v,fPET) [-]

315

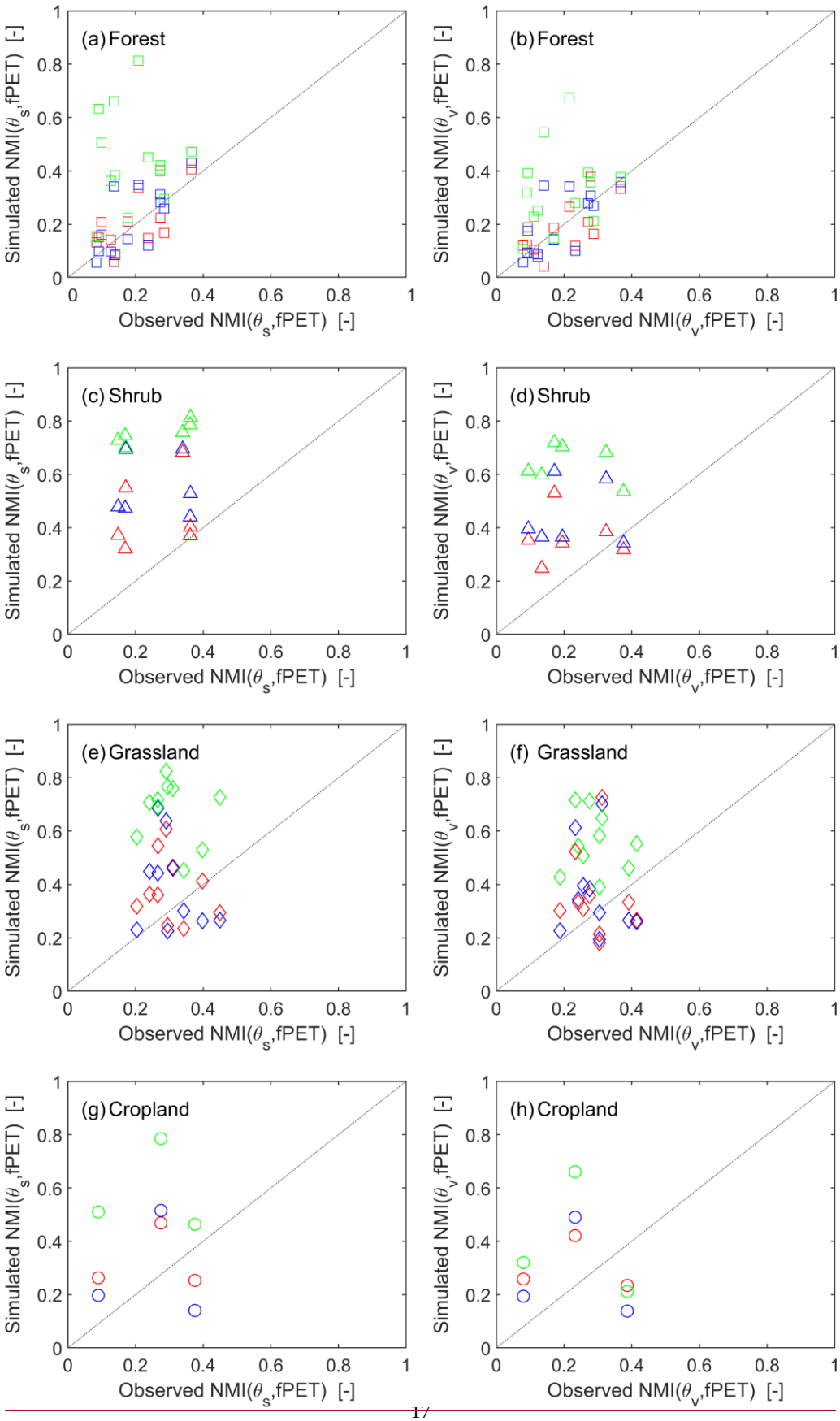
(a) Forest
(b) Forest
(c) Shrub
(d) Shrub
(e) Grassland
(f) Grassland
(g) Cropland
(h) Cropland
Simulated NMI(θ_s,fPET) [-]
Observed NMI(θ_s,fPET) [-]
Simulated NMI(θ_v,fPET) [-]
Observed NMI(θ_v,fPET) [-]
0
0.2
0.4
0.6
0.8
1

316

Fig. 4 Scatterplot of LSM-based and GLEAM-based (a) NMI(θ_S, fPET) and (b) NMI(θ_V, fPET) results versus AmeriFlux observations. Red symbols represent simulations from NOAHMP36; blue symbols represent simulations from CLSM2 and green symbols represent GLEAM retrievals.

3.4 Sensitivity of NMI(θ_S, fPET)/NMI(θ_V, fPET) ratio to climatic conditions

Figure 5 further summarizes the ~~ratio of~~ NMI(θ_S, fPET) ~~and~~ /NMI(θ_V, fPET) ratio as a function of AI for all four products (NOAHMP, CLSM, GLEAM and AmeriFlux). Error bars represent the standard deviation of sampling errors calculated from a 500-member bootstrapping analysis. With increasing AI, there is a significant decreasing trend in ~~surface and vertically integrated θ/ET coupling within~~ both NMI(θ_S, fPET) and NMI(θ_V, fPET) for all three simulations, with a goodness-of-fit above 0.5 (figure not shown). For all cases, the NMI(θ_S, fPET)/NMI(θ_V, fPET) ratios are consistently greater than unity under all climatic conditions. However, the estimated NMI(θ_S, fPET)/NMI(θ_V, fPET) ratios from all three simulations (NOAHMP, CLSM and GLEAM) exhibit quite different trends with respect to AI. The NMI(θ_S, fPET)/NMI(θ_V, fPET) ratio for CLSM decreases with increasing AI, with a moderate goodness-of-fit value of 0.28, while GLEAM estimates of NMI(θ_S, fPET)/NMI(θ_V, fPET) shows an opposite increasing trend with increasing AI. ~~both NOAHMP and CLSM. This decreasing trend is particularly clear when AI is below 1.0 [ ]. NOAHMP, CLSM and GLEAM estimates of NMI(θ_S, fPET) are generally higher than NMI(θ_V, fPET) in all climatic conditions.~~ Conversely, there~~There~~ is relatively lower sensitivity of the NMI(θ_S, fPET)/NMI(θ_V, fPET) ratio to ~~aridity~~ AI captured in the AmeriFlux measurements~~, as the NMI(θ_S, fPET)/NMI(θ_V, fPET) ratio still approximates one under semiarid conditions (i.e., AI < 0.5 [ ])~~.

Connecting these findings to spatial distribution of NMI(θ_S, fPET) and NMI(θ_V, fPET) (Fig. 3) ~~, it is~~ confirm~~ed~~ that the relative magnitudes of NMI(θ_S, fPET) and NMI(θ_V, fPET) for both~~all three~~ LSMs and GLEAM are spatially related to hydro-climatic regimes ~~(although in fundamentally different ways)~~. In contrast, this link is weaker in the AmeriFlux measurements which, except for a small fraction of very low AI sites, do not appear to vary as a function of AI. These conclusions are not qualitatively impacted by looking at NMI(θ_S, fPET) and NMI(θ_V, fPET) differences, as opposed to their ratio as in Fig. 5, or by looking at R(θ_S, fPET) and R(θ_V, fPET) instead of NMI.

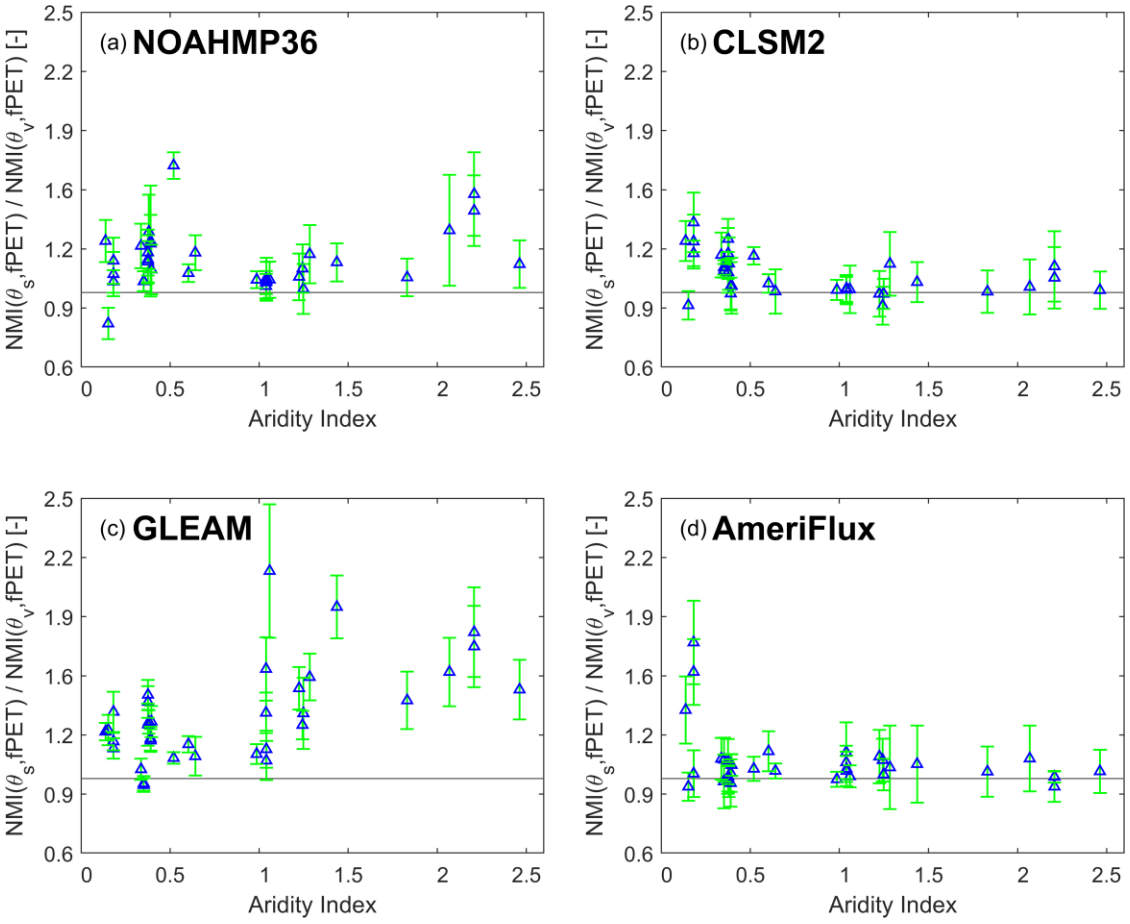

Fig. 5 For a) NOAHMP, (b) CLSM, (c) GLEAM and (d) AmeriFlux estimates, the ratio of NMI(θ_S, fPET) and NMI(θ_V, fPET) as a function of AI across all AmeriFlux sites.

4 Discussion and conclusion

Since transpiration dominates the global ET (Jasechko et al., 2013), deep-layer soil ~~moisture~~water content (θ_V) is generally considered to contain more ET information than that of surface soil ~~moisture~~water content (θ_S) – given plant transpiration is balanced by root water uptake from deeper soils (Seneviratne et al., 2010). However, this assumption is rarely tested using models and/or observations. Here, we apply normalized mutual information (NMI) to examine how the vertical support of a soil ~~moisture~~water content product ~~impacts~~affects its relationship with concurrent surface ET.

Specifically, using AmeriFlux ground observations, we examine whether (NMI-based) estimates of LSMs and GLEAM θ_S versus ET and θ_V versus ET coupling strength accurately reflect observations acquired at a range of AmeriFlux sites. In general, compared to the baseline case of exponential filter extrapolated 40-cm bottom layer θ_V, LSMs and GLEAM agree with AmeriFlux observations in that the overall fPET information contained in θ_S is slightly higher than that of θ_V (Fig. 1). However, the sensitivity analysis showed this difference between NMI(θ_S, fPET) and

NMI(θ_V, fPET) diminishes when using different methods for calculating θ_V using AmeriFlux observations (Fig. 2). As a result, this result should be viewed with caution.

While NOAHMP and CLSM derived NMI(θ_S, fPET) and NMI(θ_V, fPET) results are generally consistent with the AmeriFlux observations, GLEAM overestimates NMI(θ_S, fPET), NMI(θ_V, fPET), and the ratio NMI(θ_S, fPET)/NMI(θ_V, fPET) relative to observations. Although both LSMs and GLEAM are based on the same classical two-section (soil ~~moisture~~water content-limited and energy-limited) ET regimes framework (Sect. 2.2), they differ in two fundamental aspects. First, the evaporative stress factor S is represented as a more direct and strong function of soil ~~moisture~~water content in GLEAM - see Eqs. (4) and (5) - which leads to the overestimation of θ/ET coupling strength. This is consistent with our results that GLEAM generally overestimates NMI(θ_S, fPET) and NMI(θ_V, fPET) consistently across all land covers, compared to AmeriFlux-based estimates. On the other hand, NOAHMP and CLSM approximate ET in the manner of biophysical models, and expresses biophysical control on ET through the stomatal resistance r_s, which is a function of multiple limiting factors including θ. Therefore, the more complex ET scheme employed by NOAHMP and CLSM would seem to mitigate the overestimation of NMI(θ_S, fPET) and NMI(θ_V, fPET), as other relevant factors besides θ (such as temperature, foliage nitrogen) are also considered in determining maximum carboxylation rate V_{max} and stomatal resistance r_s - and consequently more realistic actual ET.

Second~~ly~~, the stress factor β in both LSMs considers the cumulative effects of θ conditions along different layers (Eq. (1)), while the corresponding ~~S~~ factor S in GLEAM only uses the wettest soil layer condition, which is top layer at most sites. This likely explains the overestimation of the NMI(θ_S, fPET)/NMI(θ_V, fPET) ratio by GLEAM.

Nevertheless, we would like to stress that all approaches considered in our paper contain (at their core) a parameterized relationship between θ and ET. While the implications of mis-parameterizing this relationship are arguably more severe for a land surface model, we'd argue that the issue remain relevant for any approach (such as GLEAM) that utilizes a water balance (and/or data assimilation system) approach to estimate θ and, in turn, uses θ to constrain ET. Regardless of the complexity that a given approaches employs, failing to accurately describe the relationship between ET and (large number of potential) environmental constraints should eventually degrade the robustness of the model, no matter the model is employed as a retrospective, diagnostic or predictive manner. To examine this issue directly, Fig. 6 plots the relationship between GLEAMS bias in NMI(θ_S, fPET)/NMI(θ_V, fPET) ratio versus the RMSE of daily GLEAM ET simulations for a range of AmeriFlux sites. There is a positive correlation between the two quantities - which suggests that GLEAM overestimation of θ/ET coupling during the summer may undermine the accuracy of its daily ET retrievals. It should be noted that GLEAM simultaneously overestimates both NMI(θ_S, fPET) and NMI(θ_V, fPET); however, the impact of this mis-parameterization impact on GLEAM ET accuracy is most obvious when plotted against the ratio NMI(θ_S, fPET)/NMI(θ_V, fPET).

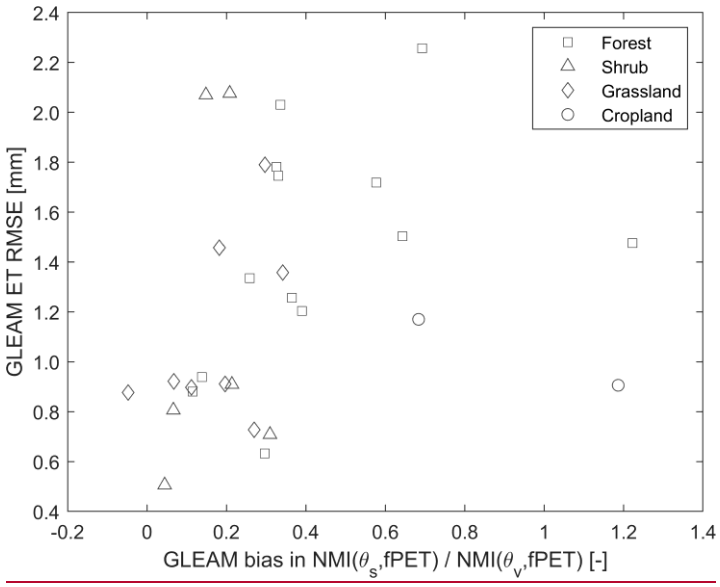

Fig. 6 Daily ET error in GLEAM as a function of GLEAM bias in NMI(θ_S, fPET)/NMI(θ_V, fPET) ratio across 34 AmeriFlux sites.

Although the median values of NMI(θ_S, fPET) and NMI(θ_V, fPET) predicted by NOAHMP and CLSM are general in line with AmeriFlux observations, they are more spatially related to hydro-climatic conditions (as summarized by AI) than their counter parts acquired from AmeriFlux measurements. Seen from the plot of NMI(θ_S, fPET)/NMI(θ_V, fPET) ratio as a function of AI (Fig. 5), the modelled and observed NMI(θ_S, fPET)/NMI(θ_V, fPET) ratio median decreases with increasing AI, and the decreasing trend is particularly clear when AI is lower than 1.0 [-]. In contrast, there is relatively lower sensitivity to aridity exhibited in the AmeriFlux measurements.

These results provide several key insights into future land-atmosphere coupling analysis and LSM as well as ET algorithm development. First, all the datasets – both model-based and ground-observed – indicates that θ_S contain at least as much ET information as θ_v. Hence, remote-sensing land surface soil ~~moisture~~water content datasets are suitable, and should be considered, for analyzing the general interaction between land and atmosphere, e.g., soil ~~moisture~~water content – air temperature coupling (Dong and Crow, 2019) and the interplay of soil ~~moisture~~water content and precipitation (Yin et al., 2014). Additionally, future generations of GLEAM may consider more sophisticated evaporation stress functions, which may improve its accuracy in representing soil's control on local ET. This may, in turn, improve the accuracy of GLEAM ET product. Finally, our results demonstrate that modeled θ/ET is ~~highly~~ more sensitive to hydro-climates~~, compared to~~ than the observed relationship~~s~~. Modifying the model structures to reduce such sensitivity might be necessary for accurately representing the interaction of land surface and atmosphere across different climate zones. This may lead to more realistic projections of future drought-induced heatwaves, when coupled with general circulation models.

Data availability

Ground-based soil ~~moisture~~water content and surface flux data are available from http://ameriflux.ornl.gov/. GLEAM dataset is available from https://www.gleam.eu/. LSMs simulations of NOAHMP and CLSM used in this study are available by contacting the authors.

Appendix A

We performed additional sensitivity analysis to explicitly demonstrate the effect of different vegetation land cover types and consequently different rooting depths (or θ_v measurement depths) on the NMI(θ_S, fPET)/NMI(θ_V, fPET) ratio, and plotted these results in Fig. A1. The figure confirms that consistent with AmeriFlux, both LSMs and GLEAM predict that NMI(θ_S, fPET) is slightly higher than NMI(θ_V, fPET) over most vegetation types, and GLEAM overestimates NMI(θ_S, fPET)/NMI(θ_V, fPET) for most vegetation types.

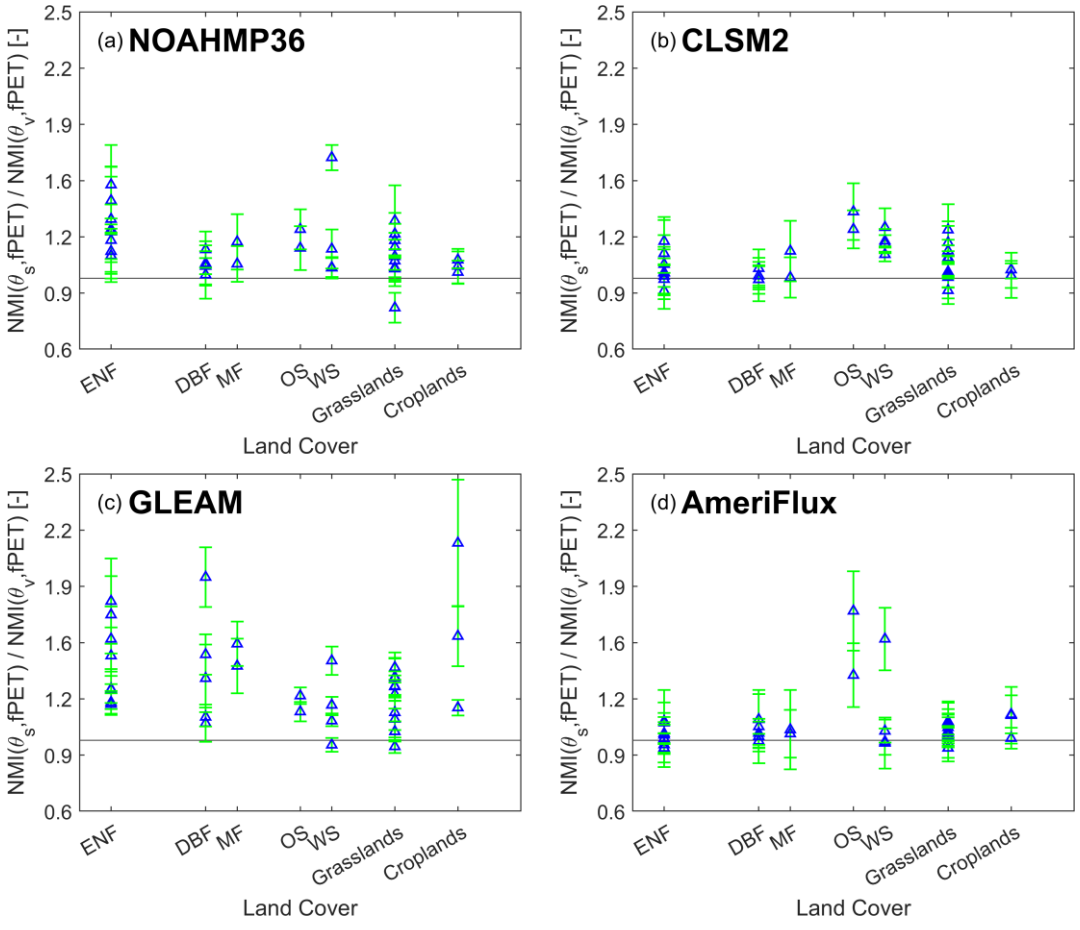

Fig. A1 For a) NOAHMP, (b) CLSM, (c) GLEAM and (d) AmeriFlux estimates, the ratio of NMI(θ_S, fPET) and NMI(θ_V, fPET) as a function of vegetation types across all AmeriFlux sites. 'ENF', 'DBF', 'MF', 'OS' and 'WS' represent evergreen needleleaf forests, deciduous broadleaf forests, mixed forests, open shrubland, and woody savannas, respectively.

Author contributions

Jianxiu Qiu and Wade T. Crow conceptualized the study. Jianzhi Dong helped preparing the LSMs simulation. Grey S. Nearing assisted in the mutual information analysis. Jianxiu Qiu carried out the analysis and wrote the first draft manuscript, and Wade T. Crow refined the work. All authors contributed to the analysis, interpretation and writing.

Competing interests

The authors declare that they have no conflict of interest.

Acknowledgments

This work was supported by National Natural Science Foundation of China (Grant Nos. 41971031, 41501450, 51779278) and Natural Science Foundation of Guangdong Province, China (Grant No. 2016A030310154).

References

Albergel, C., Rüdiger, C., Pellarin, T., Fritz, N., and Froissard, F.: From near-surface to root-zone soil moisture using an exponential filter: an assessment of the method based on in-situ observations and model simulations, Hydrol. Earth Syst. Sci., 12, 1323–1337, doi: 10.5194/hess-12-1323-2008, 2008.

Basara, J. B. and Crawford, K. C.,: Linear relationships between root‐zone soil moisture and atmospheric processes in the planetary boundary layer, J. Geophys. Res., 107, 4274, doi:10.1029/2001JD000633, 2002.

Boden, T. A., Krassovski, M., and Yang, B.: The AmeriFlux data activity and data system: an evolving collection of data management techniques, tools, products and services, Geosci. Instrum. Meth. Data Syst., 2, 165–176, doi: 10.5194/gi-2-165-2013, 2013.

Cover, T. M. and Thomas, J. A.: Elements of information theory, John Wiley & Sons, New York, 1991.

Crow, W.T., Lei, F., Hain, C., Anderson, M.C., Scott, R.L., Billesbach, D., and Arkebauer, T.: Robust estimates of soil moisture and latent heat flux coupling strength obtained from triple collocation, Geophys. Res. Lett., 42, 8415–8423, doi: 10.1002/2015GL065929, 2015.

Dirmeyer, P. A., Chen, L., Wu, J., Shin, C.‐S., Huang, B., and Cash, B. A.: Verification of land‐atmosphere coupling in forecast models, reanalyses, and land surface models using flux site observations, J. Hydrometeorol., 19, 375–392, doi: 10.1175/JHM-D-17-0152.1, 2018.

Dong, J. and Crow, W.T.: Use of satellite soil moisture to diagnose climate model representations of European soil moisture - air temperature coupling strength, Geophys. Res. Lett., 45, 12884–12891, doi: 10.1029/2018GL080547, 2018.

Dong, J. and Crow. W.T.: L-band remote-sensing increases sampled levels of global soil moisture - air temperature coupling strength, Remote Sens. Environ., 22, 51–58, doi: 10.1016/j.rse.2018.10.024, 2019.

Dong, J., Crow, W.T., Reichle, R., Liu, Q., Lei, F., and Cosh, M.: A global assessment of added value in the SMAP Level-4 soil moisture product relative to its baseline land surface model, in press, Geophys. Res. Lett., 2019.

Entekhabi, D., Njoku, E.G., O'Neill, P.E., Kellogg, K.H., Crow, W.T., Edelstein, W.N., Entin, J.K., Goodman, S.D., Jackson, T.J., and Johnson, J.: The Soil Moisture Active Passive (SMAP) mission, Proc. IEEE., 98, 704–716, doi: 10.1109/jproc.2010.2043918, 2010.

Ford, T. W., Wulff, C. O., and Quiring, S. M.: Assessment of observed and model ‐ derived soil moisture ‐ evaporative fraction relationships over the United States Southern Great Plains, J. Geophys. Res., 119, 6279–6291, doi: 10.1002/2014JD021490, 2014a.

Ford, T. W. and Quiring, S. M.: In situ soil moisture coupled with extreme temperatures: A study based on the Oklahoma Mesonet, Geophys. Res. Lett., 41, 4727–4734, doi: 10.1002/2014gl060949, 2014b.

Hirschi M., Mueller, B., Dorigo, W., and Seneviratne, S. I.: Using remotely sensed soil moisture for land–atmosphere coupling diagnostics: The role of surface vs. root-zone soil moisture variability, Remote Sens. Environ., 154, 246–252, doi: 10.1016/j.rse.2014.08.030, 2014.

Jasechko, S., Sharp, Z. D., and Gibson, J. J.: Terrestrial water fluxes dominated by transpiration, Nature, 2013, 496, 347–350, doi: 10.1038/nature11983, 2013.

Kerr, Y.H., Waldteufel, P., Wigneron, J.P., Martinuzzi, J., Font, J., and Berger, M.: Soil moisture retrieval from space: the Soil Moisture and Ocean Salinity (SMOS) mission, IEEE Trans. Geosci. Remote Sens., 39, 1729–1735, doi: 10.1109/36.942551, 2001.

Koster, R. D., Suarez, M. J., Ducharne, A., Stieglitz, M., and Kumar, P.: A catchment-based approach to modeling land surface processes in a general circulation model: 1. Model structure, J. Geophys. Res., 105, 24809–24822, doi: 10.1029/2000JD900327, 2000.

Koster, R. D., Schubert, S. D., and Suarez, M. J.: Analyzing the concurrence of meteorological droughts and warm periods, with implications for the determination of evaporative regime, J. Climate., 22, 3331–3341, doi:10.1175/2008JCLI2718.1, 2009.

Kullback, S. and Leibler, R. A.: On information and sufficiency, Ann. of Math. Stat., 22, 79–86, doi: 10.1214/aoms/1177729694, 1951.

Kumar, S. V., Peters-Lidard, C. D., Tian, Y., Houser, P. R., Geiger, J., Olden, S., Lighty, L., Eastman, J. L., Doty, B., Dirmeyer, P., dams, J.A., Mitchell, K., Wood, E. F., and Sheffield, J.: Land information system: An interoperable framework for high resolution land surface modeling, Environ. Modmell. Softw., 21, 1402–1415, doi: 10.1016/j.envsoft.2005.07.004, 2006.

Lei, F., Crow, W.T., Holmes, T., Hain, C., and Anderson, M.: Global investigation of soil moisture and latent heat flux coupling strength, Water Resources Research., 54, 8196–8215, doi:10.1029/2018WR023469, 2018.

Mahrt, L. and Ek, M.: The influence of atmospheric stability on potential evaporation, J. Clim. Appl. Meteorol., 23, 222–234, doi:10.1175/1520‐0450(1984)023<0222:TIOASO>2.0.CO;2, 1984.

Martens, B., Miralles, D. G., Hans, L., Robin, V. D. S., and de Jeu, J. R. A. M.: Gleam v3: satellite-based land evaporation and root-zone soil moisture, Geosci. Model Dev., 10, 1903–1925, doi: 10.5194/gmd-10-1903-2017, 2017.

Miralles, D. G., Holmes, T. R. H., De Jeu, R. A. M., Gash, J. H., Meesters, A. G. C. A., and Dolman, A. J.: Global land-surface evaporation estimated from satellite-based observations, Hydrol. Earth Syst. Sci., 15, 453–469, doi:10.5194/hess-15-453-2011, 2011.

Nearing, G. S., Yatheendradas. S., and Crow, W. T.: Nonparametric triple collocation, Water Resour. Res., 53, 5516–5530, doi: 10.1002/2017WR020359, 2017.

Nearing, G. S., Ruddell, B. L., Clark, M. P., Nijssen, B., and Peters-Lidard, C. D.: Benchmarking and Process Diagnostics of Land Models, J. Hydrometeorol., 19, 1835–1852, doi: 10.1175/JHM-D-17-0209.1, 2018.

Nearing, G. S., Mocko, D. M., Peters-Lidard, C. D., Kumar, S. V., and Xia, Y.: Benchmarking NLDAS-2 Soil Moisture and Evapotranspiration to Separate Uncertainty Contributions, J. Hydrometeorol., 17, 745–759, doi: 10.1175/JHM-D-15-0063.1, 2016.

Nearing, G. S. and Gupta, H. V.: The quantity and quality of information in hydrologic models, Water Resour. Res., 51, 524–538, doi: 10.1002/2014WR015895, 2015.

Nearing, G. S., Gupta, H. V. Crow, W. T., and Gong, W.: An approach to quantifying the efficiency of a Bayesian filter, Water Resour. Res., 49, 2164–2173, doi: 10.1002/wrcr.20177. 2013.

Niu, G. Y., Yang, Z. L., Mitchell, K. E., Chen, F., Ek, M. B., Barlage, M., Kumar, A., Manning, K., Niyogi, D., Rosero, E., Tewari, M., and Xia, Y. L.: The community Noah land surface model with multiparameterization options (Noah-MP): 1. Model description and evaluation with local-scale measurements, J. Geophys. Res., 116, 1248–1256, doi:10.1029/2010jd015139, 2011.

Paninski, L.: Neural Computation, Estimation of Entropy and Mutual Information., 15, 1191–1253, doi: 10.1162/089976603321780272, 2003.

Priestley, J. H. C. and Taylor, J.: On the assessment of surface heat flux and evaporation using large-scale parameters, Mon.Weather Rev., 100, 81–92, doi: 10.1175/1520-0493(1972)1002.3.CO;2, 1972.

Qiu, J., Crow, W. T., and Nearing, G. S.: The impact of vertical measurement depth on the information content of soil moisture for latent heat flux estimation, J. Hydrometeorol., 17, 2419–2430, doi: 10.1175/JHM-D-16-0044.1, 2016.

Qiu, J., Crow, W. T., Nearing, G. S., Mo, X., and Liu, S.: The impact of vertical measurement depth on the information content of soil moisture time series data, Geophys. Res. Lett., 41, 4997–5004, doi: 10.1002/2014GL06001, 2014.

Scott, D. W.: Multivariate density estimation and visualization, in Handbook of Computational Statistics: Concepts and Methods, Springer, New York, 2014.

Seneviratne, S. I., Wilhelm, M., Stanelle, T., Hurk, B., Hagemann, S., and Berg, A.: Impact of soil moisture - climate feedbacks on CMIP5 projections: First results from the GLACE - CMIP5 experiment, Geophys. Res. Lett., 40, 5212–5217, doi: 10.1002/grl.50956, 2013.

Seneviratne, S. I., Corti, T., Davin, E. L., Hirschi, M., Jaeger, E. B., and Lehner, I.: Investigating soil moisture–climate interactions in a changing climate: A review, Earth-Sci. Rev., 99, 125–161, doi:10.1016/j.earscirev.2010.02.004, 2010.

Shannon, C. E.: A mathematical theory of communication, Bell Labs Tech. J., 27, 379–423, doi: 10.1002/j.1538–7305.1948.tb00917.x, 1948.

Wagner, W., Lemoine, G., and Rott, H.: A method for estimating soil moisture from ERS scatterometer and soil data, Remote Sens. Environ., 70, 191–207, doi: 10.1016/S0034-4257(99)00036-X, 1999.

Yin, J., Porporato, A., and Albertson, J., Interplay of climate seasonality and soil moisture-rainfall feedback, Water Resour. Res., 50, 6053–6066, doi: 10.1002/2013WR014772, 2014.